JOURNAL OF MATERIALS SCIENCE 23 (1988) 723–728

Effect of strain rate on sigma formation in ferrite–austenite stainless steel at high temperatures

T. CHANDRA
Department of Metallurgy and Materials Engineering, University of Wollongong, Wollongong 2500, New South Wales, Australia

R. KUCHLMAYR
BHP Steel International, Slab and Plate Products Division, Port Kembla, New South Wales, Australia

Sigma precipitation in an Fe–19Cr–5Ni–2.7Mo ferrite–austenite duplex stainless steel has been investigated during and after uniaxial compression at 900° C. At this temperature ferrite and austenite phases are present in equivolume proportions (1 : 1). It was found that sigma precipitation was enhanced by hot working and the volume proportion of sigma decreased as the straining rate increased. Sigma nucleated at ferrite–austenite interfaces and grew into ferrite grains by the eutectoid reaction $\alpha \rightarrow \sigma + \gamma$. Transmission electron microscopy revealed that large sigma particles enhanced recrystallization of the austenite phase in duplex structures at high temperature.

1. Introduction

Sigma phase is probably the most undesirable phase that can form in duplex stainless steels [1]. Maehara and co-workers [2, 3] and Chandra *et al.* [4] have recently reported that sigma precipitation is enhanced by hot working and the rate of precipitation is dependent on both strain and prior thermal history (heat-treatment). Since hot working is generally carried out at high strain rates, it is of industrial importance to know how precipitation of deleterious sigma will be influenced by the rate of deformation at high temperatures. Such sigma precipitation greatly reduces the toughness of duplex steels and causes embrittlement at lower temperatures. The principal aim of this work was to study the effect of strain rate on sigma formation during and after high temperature deformation. The secondary purpose was also to investigate the role of sigma particles on the recrystallization behaviour of ferrite and austenite in duplex stainless steel.

2. Experimental procedures

The material used in this investigation was a commercial duplex stainless steel which has nominal composition of 0.03C, 1.5Mn, 1.7Si, 18.5Cr, 4.9Ni and 2.7Mo (wt %). The alloy 3RE60 was supplied by Sandvik (Australia) Pty Ltd in the form of hot-rolled bar of 45 mm in diameter. Rod-shaped samples, 8 mm diameter × 11 mm long, were machined in the rolling direction and were heat-treated at 900° C for 10 min and then water-quenched. This treatment produced a microstructure which consisted of 55% austenite within a ferrite matrix.

Isothermal hot compression testing was carried out on a Dartec servo-hydraulic testing machine modified for hot compression under constant straining rate. All tests were conducted in high-purity argon to minimize oxidation. Samples were held at the test temperature of 900° C for 5 min prior to compression to a true strain of 0.8 at strain rates of 1 and 0.01 sec^{-1}. After deformation, samples were aged at the test temperature for 1, 2, 5, 15, 30 and 60 min, and then water-quenched to retain the deformed structure.

The microstructures were examined by optical and scanning electron microscopy after electrolytically etching in KOH solution. Point-counting was used to determine the fractions of α, γ and σ phases as a function of ageing time. Thin-foil electron microscopy was also carried out using perchloric and acetic acid solution for thinning and polishing the specimens. The thin foils were then examined in a Jeol 100U transmission electron microscope at 120 kV.

3. Results and discussion

The true stress–true strain curves obtained during hot compression at true strain rates of 1 and 0.01 sec^{-1} at 900° C are shown in Fig. 1. The shape of these flow curves is typical of the form expected when dynamic recovery occurs: that is, the flow stress rises sharply to a maximum at low strains and then approaches a steady-state value [5, 6].

The effect of ageing at 900° C on the precipitation of sigma phase in deformed and undeformed samples has been compared in Fig. 2. Curves (a) and (b) correspond to samples deformed to a strain of 0.8 at strain rates of 1 and 0.01 sec^{-1}, respectively, while Curve (c) represents samples which have not been deformed. It can be seen that hot working enhances sigma

0022–2461/88 $03.00 + .12

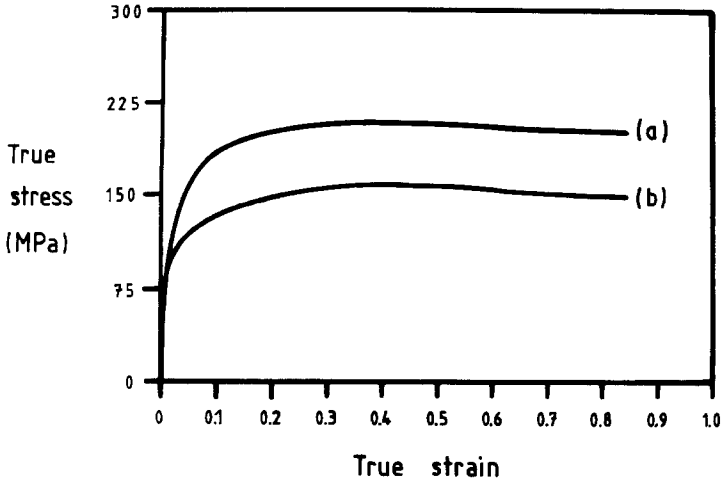

Figure 1 True stress–true strain curves for the α–γ alloy tested in compression at 900° C at strain rates of (a) 1 and (b) 0.01 sec^{-1}.

precipitation, since the two curves corresponding to the deformed samples exhibit much larger proportions of sigma phase compared to the curve for the sample in its undeformed state. For example, after a holding time of 15 min at 900° C the undeformed sample contained ~0.5% sigma phase, whereas more than 2% sigma was present in a sample deformed to true strain of 0.8 at 1 sec^{-1} and then aged for the same time of 15 min. The sample deformed to a strain of 0.8 at the lower strain rate of 0.01 sec^{-1} followed by ageing for 15 min contained ~3.5% sigma phase.

These results suggest that deformation enhances sigma formation. However, it should be noted in Fig. 2 that for ageing times greater than 15 min the volume percentage against time curve for undeformed samples merges with the curve obtained for high strain rate (1 sec^{-1}) samples. Such a merging was not observed for the samples strained at the lower strain rate of 0.01 sec^{-1}. It is evident in Fig. 2 that for the same ageing time after deformation, a significantly higher volume fraction of sigma was present in the sample strained at 0.01 sec^{-1} than for 1 sec^{-1}.

It is likely that the growth processes of sigma under slow deformation conditions differ to those in the undeformed and higher strain-rate conditions. This is probably due to several reasons. Firstly, the time required to deform a sample to a true strain of 0.8 requires approximately 1 sec at a strain rate of 1 sec^{-1}, whilst deformation at 0.01 sec^{-1} needs ~80 sec to achieve the same strain. Thus a greater volume of sigma would be expected to precipitate at lower straining rate than at high strain rate, since the sample is effectively held for a longer period in the former case. However, the large difference in volume percentage of sigma phase at these two straining rates cannot be solely attributed to such a small increase in testing time of 79 sec.

The effect of ageing at 900° C on the volume percentage of austenite is shown in Fig. 3. It can be seen that as the holding time increases the volume percentage of austenite also increases. This is consistent with the idea that two reactions are responsible for the formation of austenite: the eutectoid reaction $\alpha \rightarrow \sigma + \gamma$, and the direct decomposition of ferrite into austenite $\alpha \rightarrow \gamma$, the dominant reaction depending largely on the availability of chromium, since sigma phase is rich in chromium [3]. Chandra *et al.* [4] have shown that as more sigma phase precipitates with time, a similar increase in the volume fraction of austenite is also expected, provided the eutectoid reaction is dominant. The fact that a slightly lower volume of austenite was obtained for the slower strain rate (0.01 sec^{-1}) is probably attributable to the fact that a larger amount of sigma had precipitated, retarding the $\alpha \rightarrow \gamma$ reaction.

It seems that there are several other structural changes occurring during and after deformation

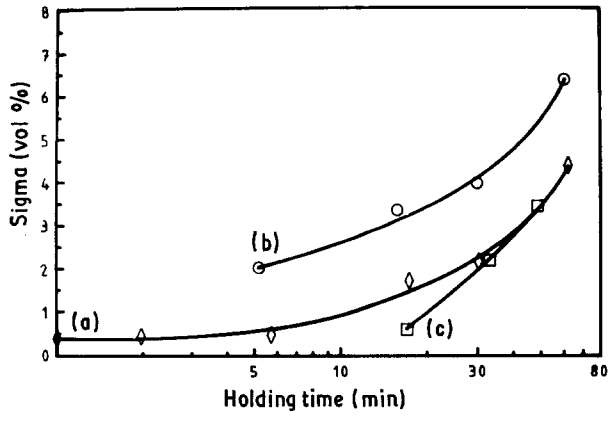

Figure 2 Volume percentage of sigma as a function of ageing time at 900° C in deformed and undeformed samples. Samples deformed to true strain of 0.8 at strain rates of (a) 1 and (b) 0.01 sec^{-1}; (c) sample in undeformed state.

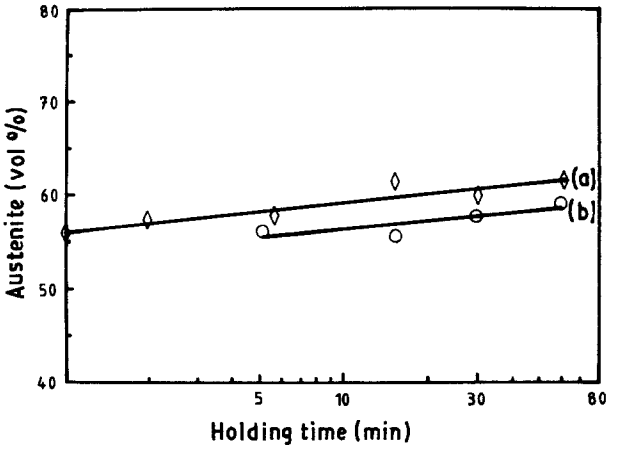

Figure 3 Volume percentage of austenite as a function of ageing time at 900° C in duplex stainless steel deformed to a strain of 0.8 at strain rates of (a) 1 and (b) 0.01 sec^{-1}.

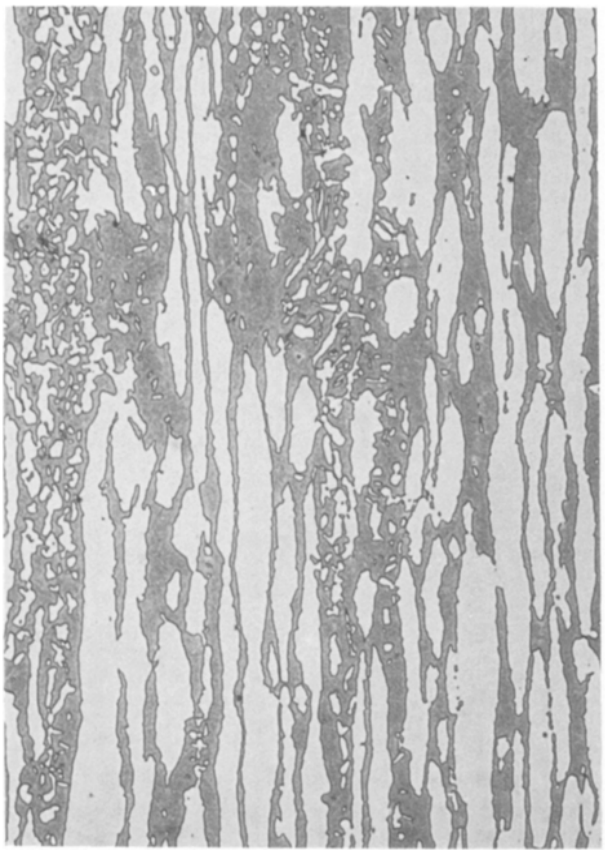

Figure 4 Microstructure of α–γ alloy solution treated at 900° C for 10 min followed by water-quenching. Structure consists of discontinuous bands of austenite (light-etched) within a matrix of ferrite (dark-etched). × 400.

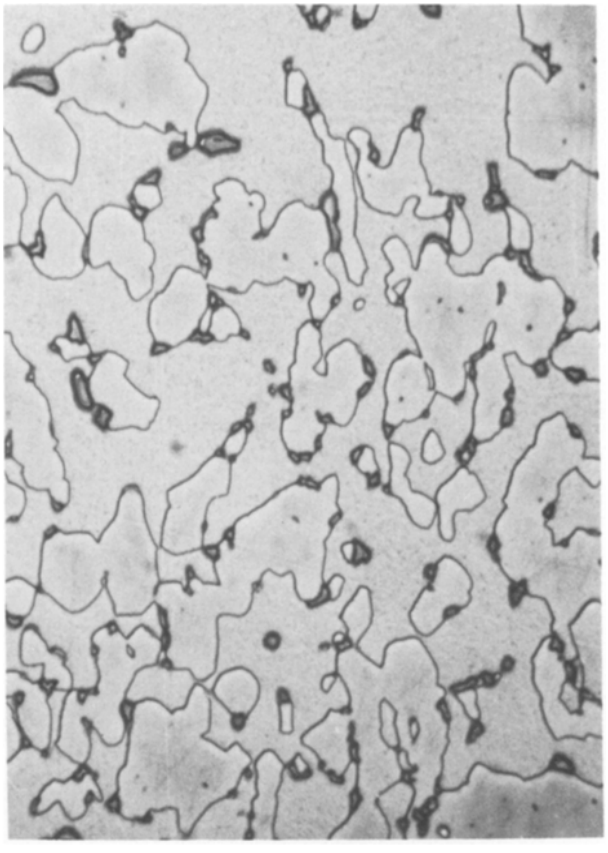

Figure 5 Microstructure of duplex alloy strained to true strain of 0.8 at 900° C at 1 sec^{-1} and then held at the test temperature for 60 min and water-quenched. Dark sigma particles can be seen at ferrite–austenite boundaries. × 650.

which may be responsible for this behaviour. Firstly, deformation at 1 sec^{-1} produces a much higher dislocation density than at 0.01 sec^{-1} at the same temperature. Thus the denser substructure at higher strain rate will result in a greater precipitation of fine sigma, due to the presence of a greater number of potent nucleating sites than at a lower strain rate. Secondly, during deformation at high strain rate the dislocation velocity will be higher so that individual dislocations will stay in contact with sigma particles for shorter periods, resulting in a lower growth of sigma particles compared to low straining rates. This effect of particle growth by pipe diffusion has been observed by Chandra *et al.* [7] and Dunlop and Honeycombe [8] in microalloyed steels. These authors suggested that a given particle coarsens by pipe diffusion until the attractive interactions with a particular dislocation diminish. The dislocation then becomes free to be entrapped by the strain field of another particle which has not yet coarsened significantly. It seems that the dislocation density and velocity of dislocations play dominant roles in determining the extent of sigma precipitation and growth at different straining rates in duplex steels during high-temperature deformation.

3.1. Microstructural characteristics

3.1.1. Optical microscopy

The as-received structure in the longitudinal direction (i.e. in the direction of rolling) consisted of discontinuous bands of austenite, known as "stringers", within a matrix of ferrite. The volume fractions of austenite and ferrite were approximately 55 and 45%, respectively. The structure resulting after solution treatment for 10 min at 900° C followed by quenching is shown in Fig. 4. This photomicrograph reveals the structure just prior to deformation. The appearance of dark-etching sigma phase within this sample suggests that sigma precipitation commences prior to deformation and then continues through deformation and subsequent ageing intervals. In other words, sigma precipitation occurs both dynamically and statically.

The severity of sigma precipitation after an ageing time of 60 min at 900° C following deformation is shown in Fig. 5. Apart from increased sigma precipitation at the ferrite–austenite interfaces, the sigma particles have also precipitated within the ferrite matrix. Two reactions have been proposed to account for this phenomenon. Firstly, it is suggested that small "islands" of austenite could have reacted to form sigma by the secondary reaction $\gamma \rightarrow \sigma$, as proposed by Maehara *et al.* [3]. The structure in Fig. 5, however, shows that many small islands of austenite remained even after an ageing time of 60 min. This would suggest that if the reaction $\gamma \rightarrow \sigma$ did occur it was very limited. It is probable that the ferrite, being rich in chromium, simply decomposed into sigma via the reaction $\alpha \rightarrow \sigma$. This reaction is feasible since the lattice rearrangement required for $\gamma \rightarrow \sigma$ is very similar to that required for $\alpha \rightarrow \sigma$. The appearance of sigma particles entirely within austenite stringers is probably misleading. This is because many of the austenite stringers exhibited small islands of ferrite phase

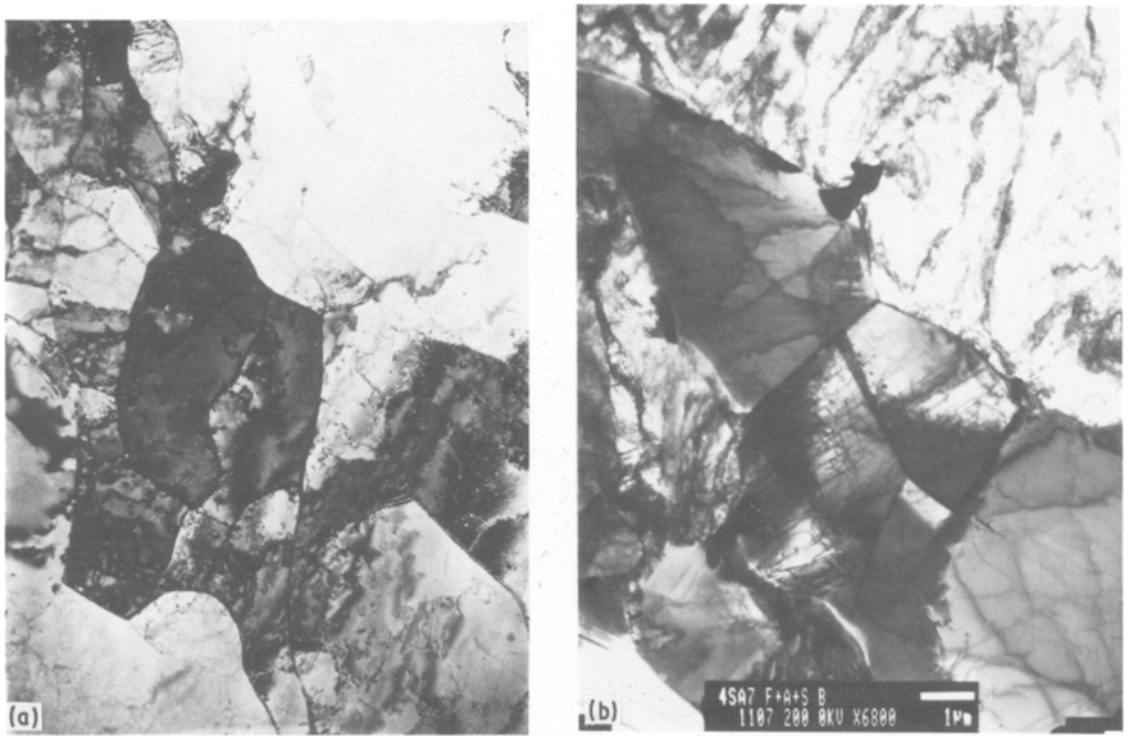

Figure 6 Transmission electron micrographs of duplex alloy aged for 1 min at 900° C after deformation to a strain of 0.8 at strain rates of (a) 1 and (b) 0.01 sec^{-1}. A well-defined substructure of ferrite can be seen at these strain rates. Note that the bulk of the austenite phase remained unrestored for short ageing periods. × 56 000.

which undoubtedly could transform to sigma via the eutectoid reaction.

3.1.2. Electron microscopy

Figs 6a and b show electron micrographs of structures of samples aged for 1 min at 900° C after deformation to a strain of 0.8 at strain rates of 1 and 0.01 sec^{-1}, respectively. It can be seen that ferrite had recovered as revealed by the well-defined substructure at both strain rates. It is possible that such recovery was mainly dynamic since the ferrite phase is of high stacking-fault energy and recovers very rapidly. The ferrite substructure did not show any observable difference with increased ageing time.

The restoration of austenite in the sample deformed at a strain rate of 1 sec^{-1} occurred mainly through static recrystallization at isolated places, although the bulk of the austenite remained unrestored for short ageing times. However, for the samples deformed at the lower strain rate (0.01 sec^{-1}) it was observed that the austenite had begun to recover dynamically as noted by the distinctive cellular substructure. Such recovery was in conjunction with the subsequent static recrystallization. This dynamic recovery is probably due to the fact that at lower straining rates the dislocations have a greater time to rearrange themselves into the more energetically favourable cellular structure, even though austenite is a phase of low stacking fault energy (SFE).

The structures of samples aged for 5 min at 900° C after deformation to a strain of 0.8 for straining rates of 1 and 0.01 sec^{-1} are shown in Figs 7a and b, respectively. In the sample strained at the high straining rate (1 sec^{-1}) it was found that sigma precipitated mainly at the ferrite–austenite boundaries and grew into the ferrite, as was observed in the samples examined optically; the sigma particle is not exactly touching the interphase boundary, and it is suggested that the boundary has migrated after nucleation. Thus, sigma particles of size $\approx 1.5\,\mu m$ in diameter seem incapable of pinning interphase boundaries. On the other hand, in the sample deformed at the lower straining rate (0.01 sec^{-1}) it was observed that sigma precipitation was far more prolific, and had also occurred along the recovered austenite sub-boundaries in addition to the ferrite–austenite interfaces. This suggests that sigma precipitation is aided by the recovery of the austenite. One possible reason for this observation may be that the solute redistribution along the low-angle boundaries occurs at a different rate compared to solute redistribution along dislocations. It has been suggested by Haessner *et al.* [9] that the movement of grain boundaries through the precipitate actually increases the coarsening of the precipitate particles, but the growth of precipitates depends on factors such as temperature, type of the interface, particle–interface energy and contact time of the particle with the interface. At high strain rates the recrystallizing interface moves more rapidly and the particles have much less residence time with such an interface. However, for lower strain rates the austenite is able to recover, providing an increase in low-angle boundaries which would increase particle residence and result in a much larger particle and volume fraction of precipitate.

Figs 8a and b correspond to the typical structures obtained for samples aged for 60 min at 900° C after deformation at 1 and 0.01 sec^{-1}, respectively. In both cases such a holding period resulted in the static recrystallization of austenite. The important point to

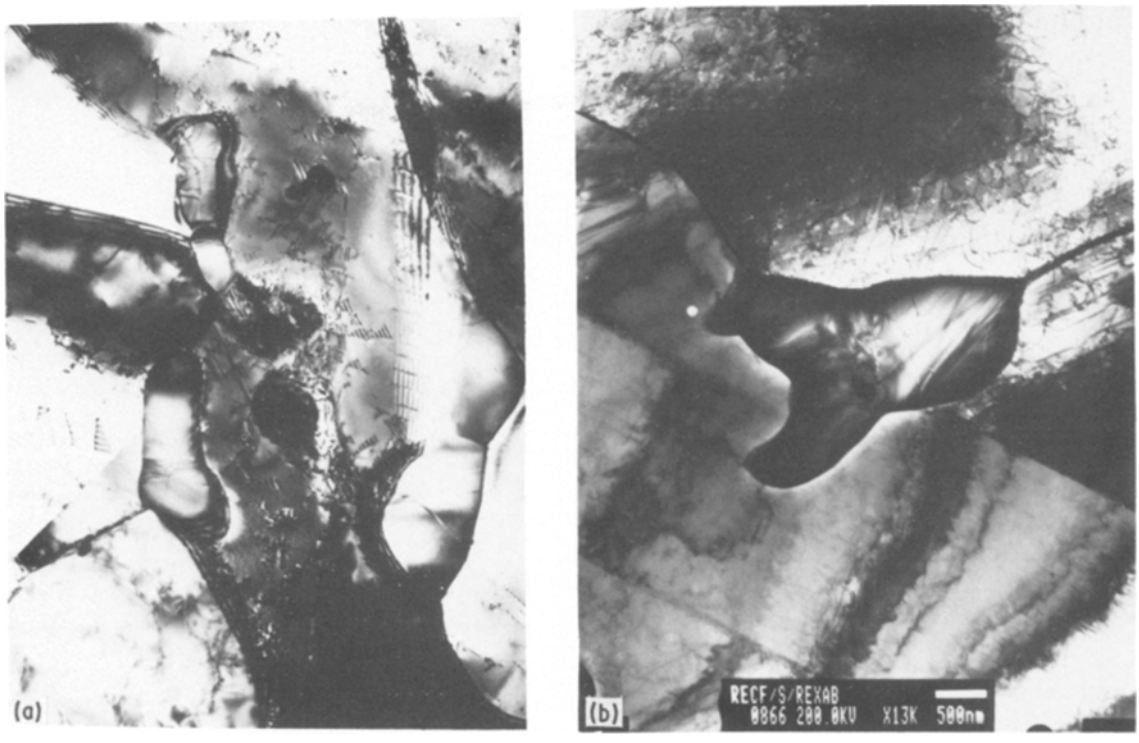

Figure 7 Transmission electron micrographs of samples aged for 5 min at 900° C after deformation to a strain of 0.8 at strain rates of (a) 1 and (b) 0.01 sec^{-1}. Ferrite is well recovered and austenite appears twinned within its grains. Dark particles of sigma can be seen at ferrite–austenite boundaries. × 56 000.

note is that the recrystallized austenite was always associated with at least one sigma particle along its interface with the recovered ferrite. This would suggest that the presence of sigma somehow triggers enhancement of austenite recrystallization. The reason for such an enhancement can be explained in terms of the large strain fields associated with sigma particles. That is, as sigma precipitates at an unrecrystallized ferrite–austenite boundary it increases the local strain in the immediate vicinity of the particle–matrix interface. As these particles grow or increase in number, the strain reaches the critical strain required for recrystallization and the austenite recrystallizes [10]. The extent of this strain field is shown by the many strain-induced features, such as twins in the recrystallized austenite and dislocation arrays within the recovered ferrite, which were commonly observed adjacent to sigma particles.

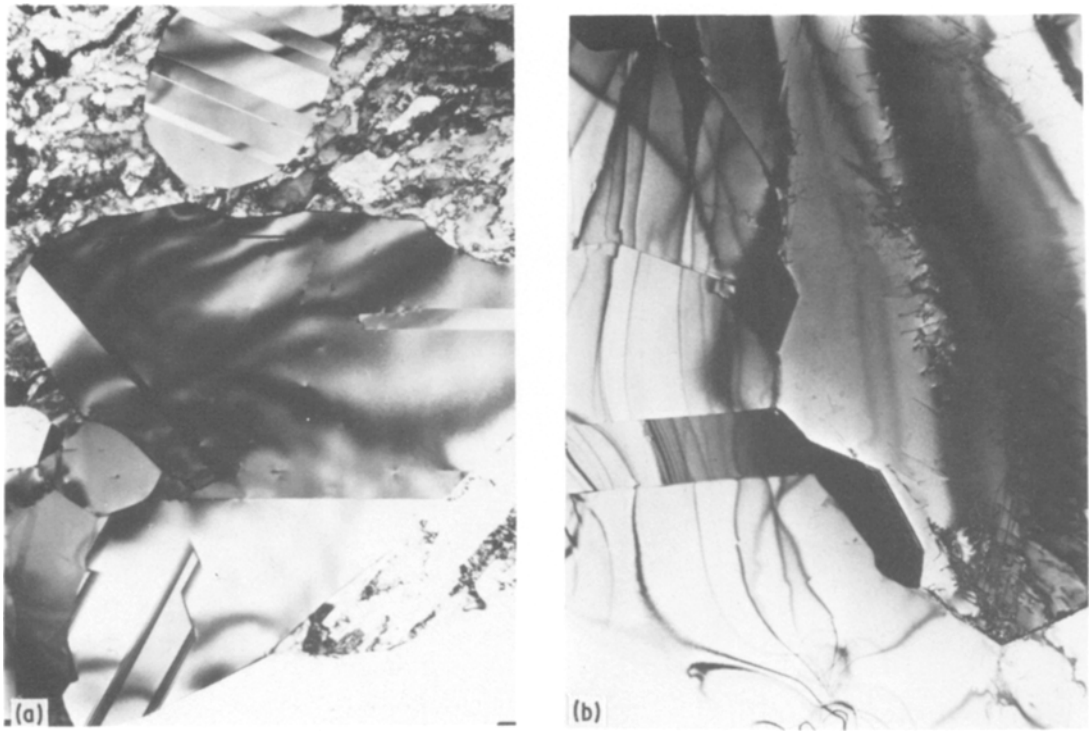

Figure 8 Transmission electron micrographs of duplex alloy aged for 5 min after deformation to a strain of 0.8 at 900° C at strain rates of (a) 1 and (b) 0.01 sec^{-1}. Recrystallized twinned austenite grains and dark sigma lie at the phase boundaries. × 82 000.

4. Conclusions

1. Precipitation of sigma phase was enhanced by hot working at 900° C. This enhancement can be explained in terms of the lattice defects introduced during deformation which act as nucleation sites for sigma precipitation.

2. The volume fraction of sigma increased as the straining rate at 900° C was decreased. This is probably attributable to the longer time required to deform a sample at a low straining rate, combined with the recovered austenite structure providing a path of less resistance to the diffusion of solute atoms.

3. Sigma precipitates were observed to nucleate at the ferrite–austenite boundaries and then grow into the ferrite phase by the eutectoid reaction $\alpha \rightarrow \sigma + \gamma$. Nucleation of sigma phase along ferrite–ferrite boundaries suggests that direct decomposition, $\alpha \rightarrow \sigma$, may also occurring. The decomposition of austenite by the reaction $\gamma \rightarrow \sigma$ was not observed.

4. Sigma precipitation enhances the recrystallization of austenite. This may be due to the large strain field associated with the sigma phase particles.

Acknowledgements

The authors wish to thank Dr I. Ward, Sandvik (Australia) Pty Ltd, for the materials used in this investigation. Special thanks are also due to Dr R. H. Edwards, BHP Steel International Group, for the use of their electron microscope unit.

References

1. H. D. SOLOMON and T. M. DEVINE, "Duplex Stainless Steels", edited by R. A. Lula (TMS–ASM, USA, 1983) p. 693.
2. Y. MAEHARA, N. FUJINO and T. KUNITAKE, *Trans. Iron Steel Inst. Jpn* **23** (1983) 247.
3. Y. MAEHARA, M. KOIKE, N. FUJINO and T. KUNITAKE, *ibid.* **23** (1983) 240.
4. T. CHANDRA, D. BENEDEICH and D. P. DUNNE, in Proceedings of International Conference on Strength of Metals and Alloys, Melbourne, 1982, edited by R. C. Gifkins (1982) 505.
5. F. E. AL-JOUNI and C. M. SELLARS, in Proceedings of 4th Riso International Symposium on Metallurgy and Material Science, Rosklide, Denmark, 1983, edited by J. B. Bilde-Sorensen (1983) 131..
6. J. J. JONAS, C. M. SELLARS and W. J. McG. TEGART, *Metall. Rev.* **14** (1969) 1.
7. T. CHANDRA, I. WEISS and J. J. JONAS, *Met. Sci. J.* **16** (1982) 97.
8. G. L. DUNLOP and HONEYCOMBE, *Phil. Mag.* **32** (1975) 61.
9. F. HAESSNER, E. HORNBOGEN and M. MUKHERJEE, *Z. Metallkde* **57** (1966) 270.
10. U. KÖSTER, *Met. Sci. J.* **8** (1974) 151.

Received 15 May
and accepted 22 July 1987